Journal of Digital Imaging (2023) 36:911–922
https://doi.org/10.1007/s10278-023-00778-0

Development and Validation of CT-Based Radiomics Signature for Overall Survival Prediction in Multi-organ Cancer

Viet Huan Le[1,2] · Quang Hien Kha[1] · Tran Nguyen Tuan Minh[1] · Van Hiep Nguyen[1,3] · Van Long Le[1,4] · Nguyen Quoc Khanh Le[5,6,7]

Received: 7 July 2022 / Revised: 11 January 2023 / Accepted: 12 January 2023 / Published online: 30 January 2023

Abstract

The malignant tumors in nature share some common morphological characteristics. Radiomics is not only images but also data; we think that a probability exists in a set of radiomics signatures extracted from CT scan images of one cancer tumor in one specific organ also be utilized for overall survival prediction in different types of cancers in different organs. The retrospective study enrolled four data sets of cancer patients in three different organs (420, 157, 137, and 191 patients for lung 1 training, lung 2 testing, and two external validation set: kidney and head and neck, respectively). In the training set, radiomics features were obtained from CT scan images, and essential features were chosen by LASSO algorithm. Univariable and multivariable analyses were then conducted to find a radiomics signature via Cox proportional hazard regression. The Kaplan–Meier curve was performed based on the risk score. The integrated time-dependent area under the ROC curve (iAUC) was calculated for each predictive model. In the training set, Kaplan–Meier curve classified patients as high or low-risk groups (p-value < 0.001; log-rank test). The risk score of radiomics signature was locked and independently evaluated in the testing set, and two external validation sets showed significant differences (p-value < 0.05; log-rank test). A combined model (radiomics + clinical) showed improved iAUC in lung 1, lung 2, head and neck, and kidney data set are 0.621 (95% CI 0.588, 0.654), 0.736 (95% CI 0.654, 0.819), 0.732 (95% CI 0.655, 0.809), and 0.834 (95% CI 0.722, 0.946), respectively. We believe that CT-based radiomics signatures for predicting overall survival in various cancer sites may exist.

Keywords Radiomics signature · Lung cancer · Head and neck cancer · Kidney cancer · Multivariable analysis · Prediction model

Introduction

The incidence of cancers has increased significantly in recent years, and cancers are the leading cause of mortality in most countries [1]. Lung cancer, with 85% being non-small cell lung cancer (NSCLC) cases, is the leading cause of neoplasm-related deaths, accounting for 18% of the mortality rate globally [1, 2]. Renal cell carcinoma (RCC), which accounted for more than 2% of all cancers and caused 179,368 deaths world-level in 2020, is currently the second most prevalent cancer of the urogenital system [1]. Head and neck cancers, with the majority of squamous cell carcinoma (HNSCC), cause the deaths of 177,757 people out of 377,713 new cases reported, especially in the low Human Development Index (HDI) countries [1]. Despite the development of tools assisting early diagnosis, improving the outcome with new therapies, the survival rates of NSCLC [2, 3], RCC [4], HNSCC [1, 5], and other types of cancer remain alarmingly low when they come to final stages of metastasis. As a result, prognostic stratification is critical

✉ Nguyen Quoc Khanh Le
khanhlee@tmu.edu.tw

1 International Ph.D. Program in Medicine, College of Medicine, Taipei Medical University, Taipei 110, Taiwan

2 Department of Thoracic Surgery, Khanh Hoa General Hospital, Nha Trang 65000, Vietnam

3 Oncology Center, Bai Chay Hospital, Quang Ninh 20000, Vietnam

4 Department of Anesthesiology and Critical Care, Hue University of Medicine and Pharmacy, Hue University, Hue City 52000, Vietnam

5 Professional Master Program in Artificial Intelligence in Medicine, College of Medicine, Taipei Medical University, Taipei 106, Taiwan

6 Research Center for Artificial Intelligence in Medicine, Taipei Medical University, Taipei 106, Taiwan

7 Translational Imaging Research Center, Taipei Medical University Hospital, Taipei 110, Taiwan

for classifying patients and assisting clinicians in making treatment options.

Medical imaging techniques have emerged to become robust, precise, yet efficient non-invasive tools for cancer diagnosis and prognosis. Medical images can now be extracted into quantitative features for further analyses of tumor properties, term "radiomics" [6–8]. Radiomics can provide personalized information for different types of cancers in other organs based on plenty of features extracted [7, 9, 10]. Quantitative features extracted from medical images play a pivotal role in evaluating distinct characteristics of malignant lesions and the regional differences of tumors. For this task, several recent studies show the superiority of models assembled by radiomics features in cancer diagnosis over conventional approaches [11–13]. Some studies focusing on radiomics features have been conducted to predict the survival outcome on NSCLC [14–16], HNSCC [17, 18], and RCC patients [4, 19]. Given the high performance of survival prediction, several radiomics signatures were used for different types of cancers. Features about tumor shape, size, intensity, and texture give phenotype information and are also used in survival analyses when combined with clinical details of the patients [7, 20].

The malignant tumors in nature share plenty of morphological characteristics, such as rough and invasive-tend boundaries, irregular shape, large volume, rapidly increasing size, vascular proliferation, and with or without tumor necrosis [21]. These common characteristics of cancerous tumors can also be detected in medical images, such as the margin's shape, size, and signs of cancerous necrosis included in the reporting and data system (-RADS), which is the imaging-based diagnostic system standardized for tumors from different organs [22]. In several recent studies, some authors have focused on the similarity of radiomics features between tumor structures in different organs and how these similarities contribute to predicting survival. How about cancer patients in different organs? Aerts et al. [23] applied one prognostic radiomics signature encompassing four radiomics features to stratify NSCLC patients into high-risk and low-risk groups, and these signatures subsequently had a significantly high performance on other NSCLC datasets and two external sets, including HNSCC patients. One study in 2019 [24] used features extracted from 2-dimensional (2D) and 3-dimensional (3D) medical images to prognose the survival probability of patients with three different malignancies. However, the NSCLC-radiomic-signature ensembled by Lee et al. [25] failed to perform a significant survival prediction on brain and kidney cancer datasets.

Based on the references mentioned above, we hypothesize whether there is one radiomics signature that can be used for the survival prediction task on different types of malignant tumors. In this study, we propose one CT-based radiomics signature that can be utilized to conduct the survival prediction analysis on NSCLC, HNSCC, and kidney cancer.

Materials and Methods

The overall study design is shown in Fig. 1.

Patient Cohort

The imaging and clinical information of the patients in this multi-cohort study was retrospectively collected from The Cancer Imaging Archive (TCIA) [26]. The institutional review board (IRB) and patient consent were waived due to the public design of this study. Four different patient cohorts are retrieved and used as follows:

1. The first cohort, lung 1 (NSCLC-Radiomics), was uploaded on TCIA, Public Access on July 2, 2014, and included 422 NSCLC patients treated at MAASTRO Clinic (Maastricht, The Netherlands) [23]. We chose 420 patients for the training set in this study due to missing information.
2. The second cohort, lung 2 (NSCLC Radiogenomics), was released to the public on TCIA, December 22, 2015, containing 211 NSCLC patients treated at Stanford University Medical Center and Palo Alto Veterans Affairs Healthcare System, USA [27]. We picked 157 patients for the testing set owing to the missing information of radiomics features.
3. Patients with HNSCC were the third dataset released July 25, 2019 (MAASTRO Clinic, (Maastricht, The Netherlands), from TCIA consisting of 137 HNSCC patients [23]. This data set was used as the first external validation.
4. The fourth dataset contains 210 patients with CT scans and segmentations from subjects from the training set of the 2019 Kidney and Kidney Tumor Segmentation Challenge (KiTS19) from University of Minnesota Health, USA [28], which was published on TCIA, Public Access on December 18, 2019. Only 191 patients were included in our study whose post-operative surgical pathology report revealed that the tumor was RCC for second external validation [28].

All of the data sets contain clinical information, such as age, gender, stage, and overall survival outcomes. Table 1 shows the baseline characteristics of patients as well as CT image data. We also listed all the subject's identifiers of each cohort in Supplementary Table S1.

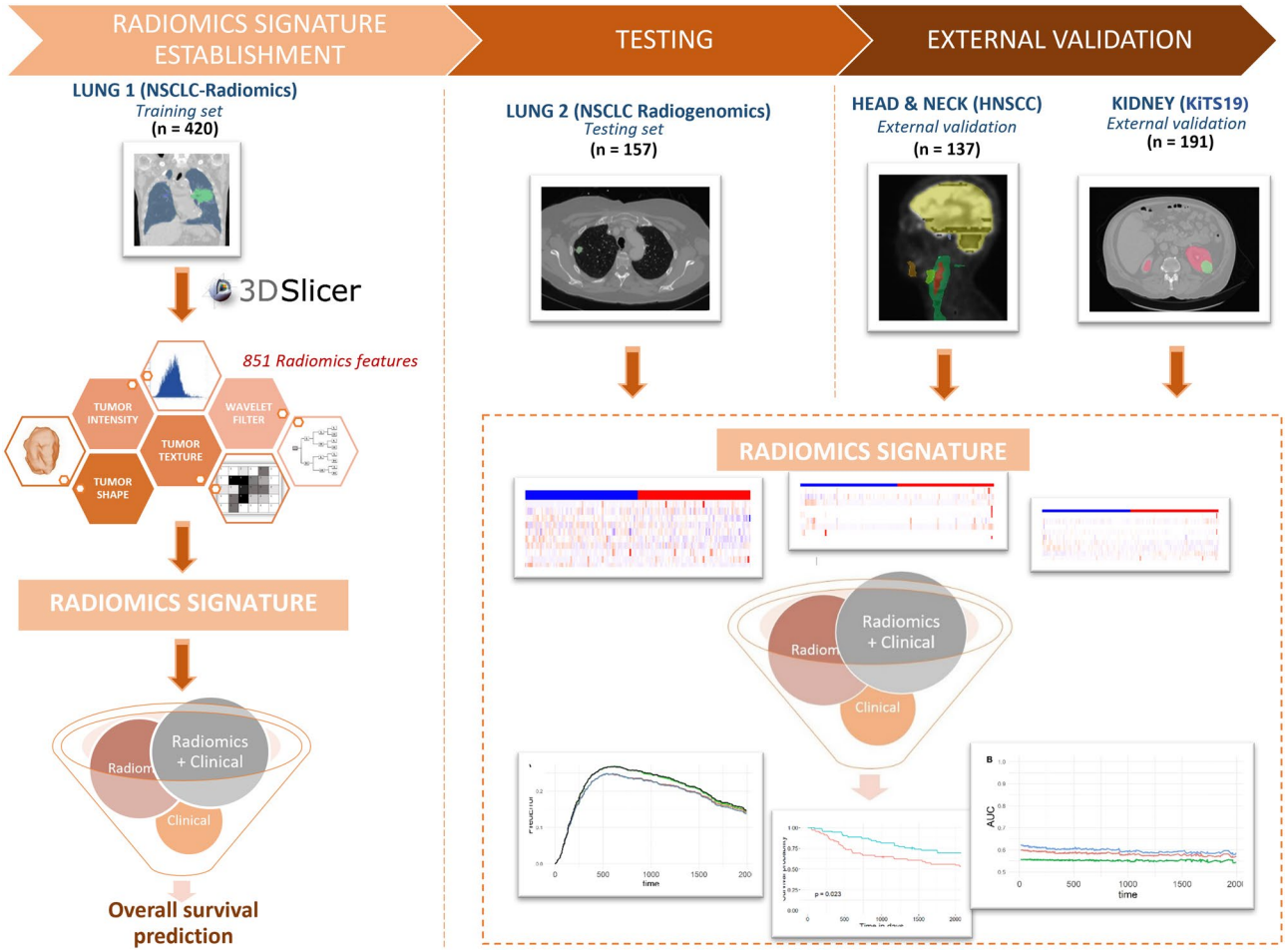

Fig. 1 Flow chart of identified CT-based radiomics signatures uniform for overall survival prediction

Radiomics Feature Extraction

Tumor segmentation was performed by the author of the datasets with CT scan images coming from different institutes and different image preprocessing (Table 1). The extraction of radiomics features from CT images in this work was implemented using 3D Slicer software [29]. To extract radiomics characteristics that satisfied the IBSI standards, the Pyradiomics library in Python was employed. Customizing bin width is set at 25; in each set of CT images of one patient, we obtained 851 radiomics features, which can be split into four categories dubbed tumor intensity, shape, texture, and wavelet filters.

Feature Selection and Best Model Construction

In the training set, pairwise correlations were performed to eliminate redundant radiomics features and avoid over-fitting or bias during analysis. The LASSO regression model is used to find the top important features [30]. Univariable Cox proportional hazard models were constructed on radiomics features refined by LASSO to find the radiomics signatures. Risk scores were calculated by the following formula [30–32]:

$$Risk\ Score = \sum_{i=1}^{n} (\beta \times \text{radiomics signature value})$$

where n denotes the number of radiomics signature features, and β is regression coefficient of each radiomics signature computed by the multivariable Cox proportional hazard model. Finally, to validate the robustness of the risk score for the survival prediction task, we applied it to the testing and two external validation sets.

Assess the Radiomics Signature and Clinical Parameter Integration's Effectiveness

For the purpose of evaluating the effectiveness in predicting survival, we combined models to evaluate survival prognosis, including clinical parameters (age, gender, stage) and

Table 1 Summary of four data sets

	Training set	Testing set	External validation set 1	External validation set 2
	TCIA—NSCLC radiomics Lung 1 ($n=420$)	TCIA—NSCLC radiogenomics Lung 2 ($n=157$)	TCIA – head-neck-radiomics-HN1 Head & neck ($n=137$)	TCIA – KiTS19 Kidney ($n=191$)
Modality	Lung CT scan	Lung CT scan	Head & Neck CT scan	Abdomen CT scan
Slice thickness (mm)	3 mm	0.625 to 3 mm	3 mm	1 to 5 mm
Segmentation algorithm	Manual delineation	Automatic segmentation and reviewed and edited by a thoracic radiologist	Manual delineation	Manual delineation
Age (mean SD)	68.01 (10.08)	68.97 (9.52)	61.96 (8.76)	58.06 (14.25)
Gender men (%)	289 (68.8)	109 (69.4)	111 (81.0)	117 (61.3)
Stage (%)	-			
Tis	0	6 (3.8)	0	0
I	92 (22.0)	104 (66.2)	24 (17.5)	128 (67.0)
II	40 (9.5)	22 (14.0)	11 (8.0)	41 (21.5)
IIIa	111 (26.5)	16 (10.2)	23 (16.8)	2 (1.0)
IIIb	176 (42.0)	5 (3.2)		
IVa	0	4 (2.5)	68 (49.6)	20 (10.5)
IVb			10 (7.3)	
IVc			1 (0.7)	
Overall survival time (median (IQR)) (days)	548.00 (260.25, 1414.25)	1315.00 (630.00, 1921.00)	2,778.00 (912.00, 3198.00)	800.00 (275.00, 1410.50)

radiomics signatures model. We compared the performance of the models against each other and to find the best model in predicting survival [33, 34].

Statistical Analysis

Before constructing the model, all radiomics features were normalized using the z-score normalization. We employed Pearson's correlation analysis to measure the correlation of every radiomics feature pairs in the training set [35, 36]. If the correlation coefficient between two features is greater than 0.7, which illustrated a high correlation, we determined to exclude one with lower correlation coefficient to the survival outcome and retain the more significant one. Top feature importance was found by LASSO regression model using the "*glmnet*" package. Risk score for each patient was calculated using the best model radiomics signatures by the Est.PH function in the "*survC1*" package. The Kaplan–Meier curve was plotted to visualize the stratification of patients as high- or low-risk group following the median risk score. The iAUC was obtained for each predictive model using the "*risksetROC*" and "*SurvC1*" package. Bootstrapped resampling with 1000 repetitions was used to calculate the differences in iAUC between the multivariable predictive models; if the 95% CI of the iAUC difference did not contain a zero value, the difference was judged statistically significant. Risk prediction abilities were assessed by graphing the Brier score prediction error curves across survival times by the "*pec*" package in R [33, 34, 37, 38]. All analyses were performed in R (version 3.3.0) and Python (version 3.8). We defined "statistical significance" as the p-value of the measurement less than 0.05.

Results

Patient's Characteristics

The four data sets in this study are extracted from TCIA which are information about cancer patients from three different organ locations: lung, kidney, and head and neck. The mean age of patients is lung 1 training set 68.01, lung 2 testing set 68.97, head and neck validation set 61.96, and kidney validation set 58.06. The male gender predominates in all data sets. The majority of the lung 1 training set was stage IIIb; accounting for 42%, the lung 2 testing set was stage I (66.2%). Similarly, the kidney validation set at the stage I is predominated (67%). The head and neck validation set at stage IVa accounted for the majority, 49.6%. The shortest median overall survival time is the lung 1 training set: 548.00 days (260.25, 1414.25), and the median of the longest overall survival time is head and neck validation set 2778.00 days (912.00, 3198.00) (Table 1).

Feature Selection

After Pearson's correlation pairwise selection, 95 radiomics features were maintained in the training set; the LASSO model was created to determine the most important 15 features for predicting overall survival and continue to proceed to find radiomics feature signatures (Fig. 2).

Radiomics Signature Prognostic Model Construction

In the training set, a univariable Cox regression was built to determine radiomics signature model. Here, we acquired ten features significantly related to overall survival prediction (Table 2) (Fig. 3): original-shape-voxel-Volume (p = 4.55e-06), Original-Shape-Major-Axis-Length (p = 0.000511), Original-gldm-Large-Dependence-emphasis ($p = 0.00109$), original-first-order-energy ($p = 0.00102$), wavelet-HLL-glcm-correlation ($p = 0.00574$), wavelet-HLL-glszm-GrayLevelNonUniformityNormalized ($p = 0.000458$), wavelet-LHL-glcm-MCC ($p = 0.0332$), wavelet-LHL-first-order-skewness ($p = 0.00241$), wavelet-LLH-glcm-Cluster-Shade ($p = 0.00642$), wavelet-LLH-first-order-maximum (0.00134).

Establishment of a Risk Score for Predicting Overall Survival in the Training Set

The Cox coefficients of the ten radiomics signatures were used to produce the risk score. The median of the risk score, which has distinct expression patterns than the signatures of the radiomics characteristics, was used to separate patients into high- and low-risk groups (Fig. 3). It can be observed from the Kaplan–Meier curve (Fig. 4A) that high-risk patients experienced a diminished survival time than low-risk ones ($p < 0.0001$).

The Radiomics Signature Model for Overall Survival Prediction Was Tested and Externally Validated

From the optimal radiomics signature gained from the training process, we further assessed its predicting robustness in the testing set (lung 2) and two external validation sets (head and neck and kidney). A specific risk score for each patient in the testing and external validation set was formulated on ten radiomics signatures. In the lung 2 cohort, the Kaplan–Meier curves illustrated that patients diagnosed with high-risk NSCLC came across with a shorter survival time than ones in the low-risk group

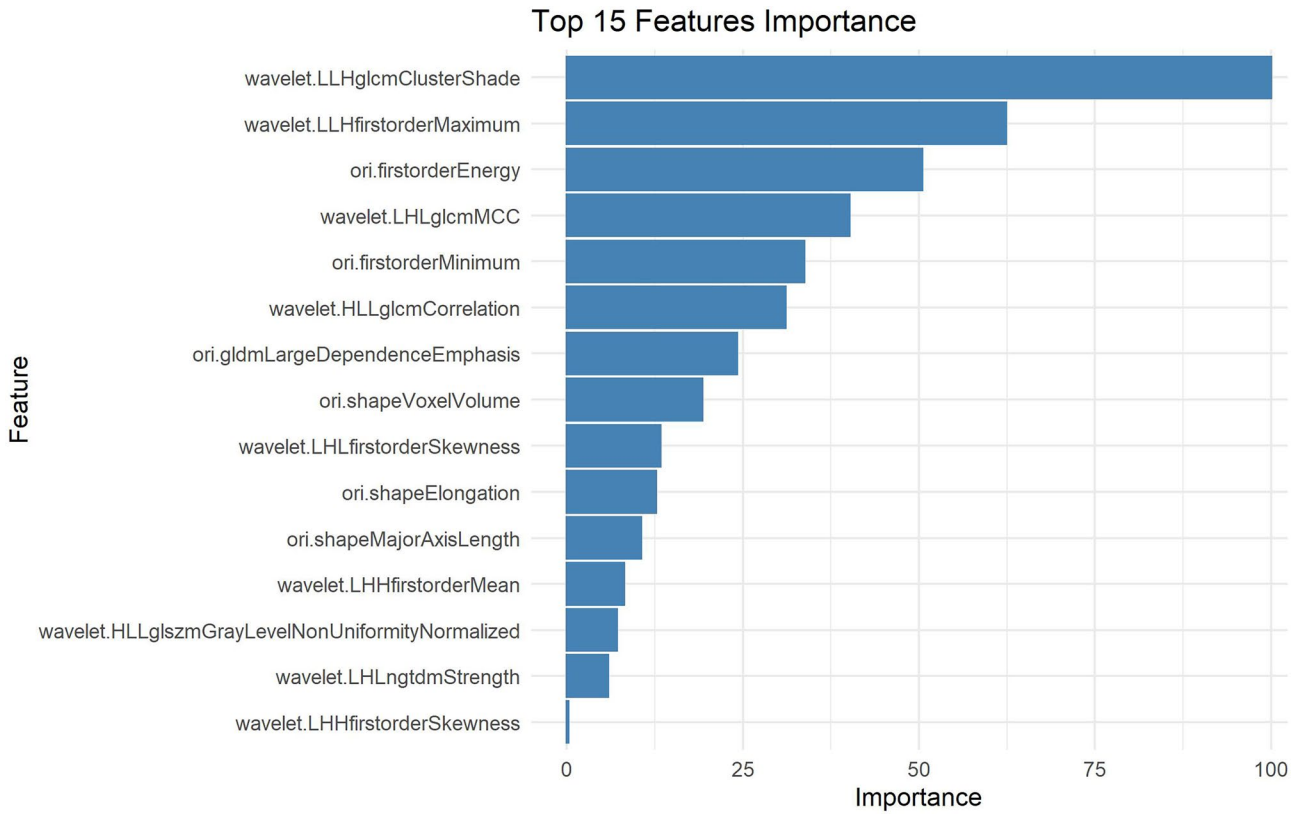

Fig. 2 Feature selection: top fifteen features selected by LASSO in the training set

Table 2 Univariable Cox regression analysis in the lung 1 training set

Feature	Hazard ratio	*p*-value	Concordance
Original shape voxel volume	1.000e + 00 (1.00–1.00)	4.55e-06 ***	0.583 (se = 0.016)
Original shape major axis length	1.005061 (1.002–1.008)	0.000511 ***	0.582 (se = 0.016)
Original shape elongation	0.7160 (0.3848–1.332)	0.292	0.517 (se = 0.017)
Original gldm large dependence emphasis	1.003723 (1.001–1.006)	0.00109 **	0.571 (se = 0.016)
Original first-order energy	1.000e + 00 (1.00–1.00)	0.00102 **	0.564 (se = 0.017)
Original first-order minimum	1.0004024 (0.9994–1.001)	0.438	0.485 (se = 0.016)
Wavelet HLL glcm correlation	0.1036 (0.02072–0.5175)	0.00574 **	0.549 (se = 0.016)
Wavelet HLL glszm GrayLevelNonUniformityNormalized	343.630 (13.11–9006)	0.000458 ***	0.551 (se = 0.016)
Wavelet LHL glcm MCC	3.4081 (1.102–10.54)	0.0332 *	0.525 (se = 0.016)
Wavelet LHL first-order skewness	0.77914 (0.6632–0.9154)	0.00241 **	0.557 (se = 0.016)
Wavelet LHL ngtdm strength	0.93152 (0.8665–1.001)	0.0545	0.571 (se = 0.017)
Wavelet LHH first-order skewness	0.98459 (0.6937–1.398)	0.931	0.499 (se = 0.017)
Wavelet LHH first-order mean	0.88519 (0.7761–1.01)	0.0692	0.531 (se = 0.016)
Wavelet LLH glcm ClusterShade	1.000e + 00 (0.9999–1)	0.00642 **	0.545 (se = 0.016)
Wavelet LLH first-order maximum	1.0005368 (1.00–1.001)	0.00134 **	0.565 (se = 0.016)

* < 0.05, ** < 0.01, *** < 0.001

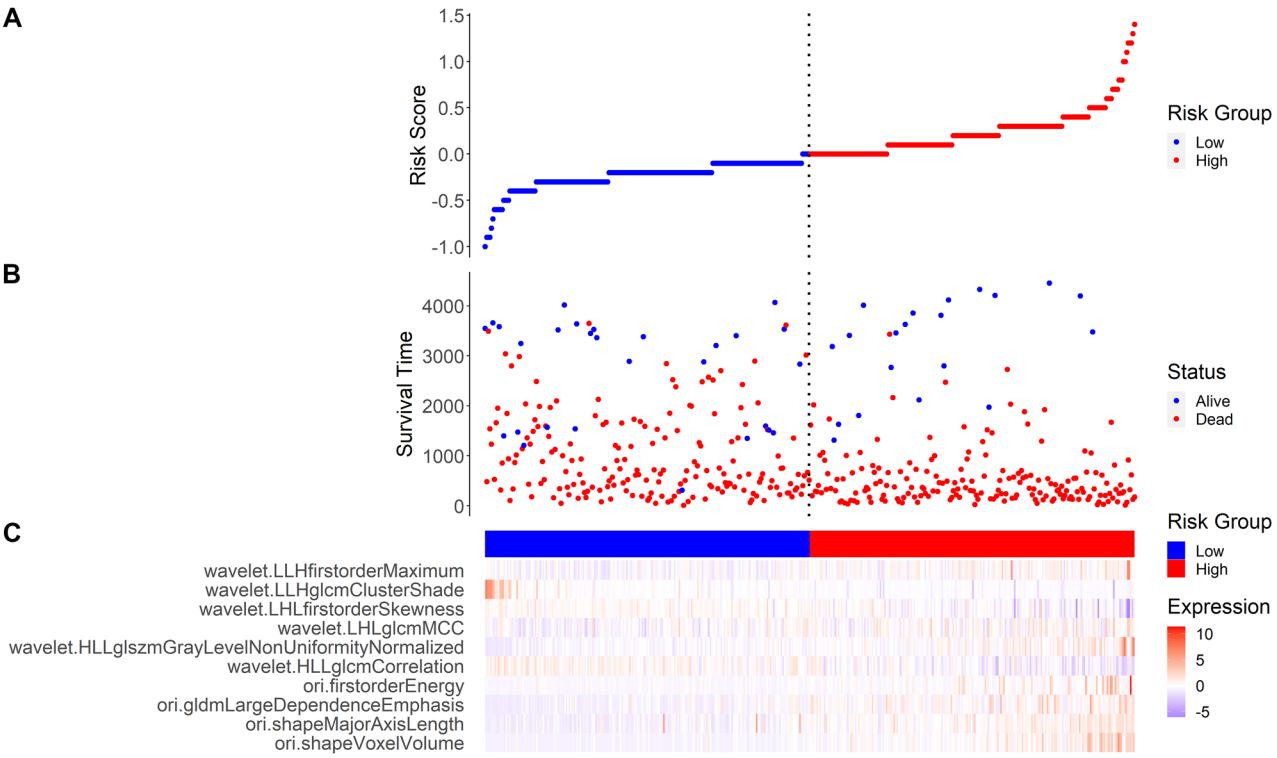

Fig. 3 Risk score distribution and ten features radiomics signatures expression in lung 1 training set. **A** Risk score distribution. **B** Two categories on the scatter plot: low-risk group (blue color) and high-risk group (red color). **C** Heat map of 10 radiomics signatures' expression

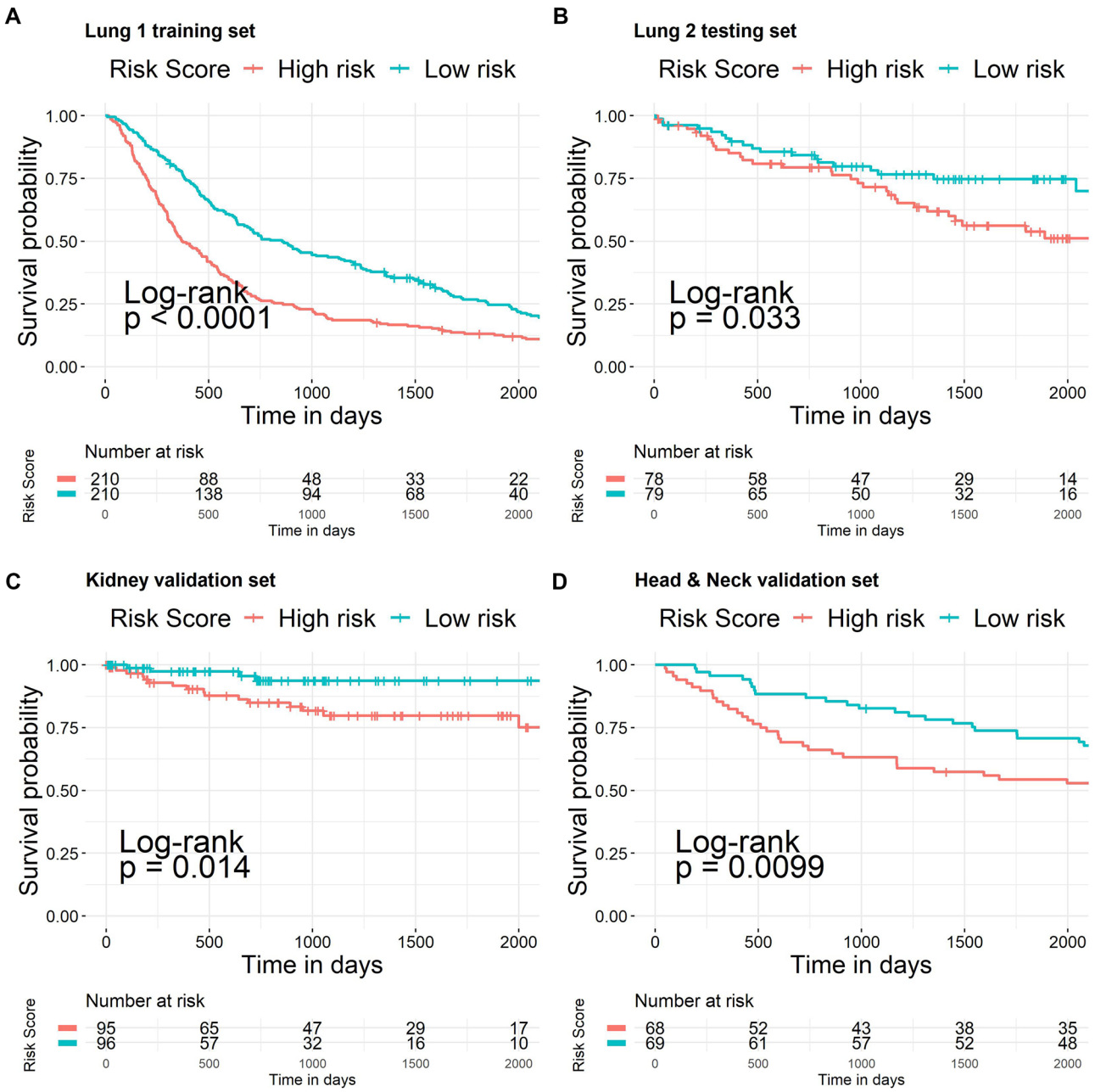

Fig. 4 Survival function of risk score generated from CT-based radiomics signatures in **A** lung 1 training set, **B** lung 2 testing set, **C** kidney validation set, and **D** head and neck validation set

($p = 0.033$) (Fig. 4B). In a similar result in the head and neck validation set and the kidney external validation set, the Kaplan–Meier curve showed that log-rank test p-value is 0.0099 and 0.014, respectively (Fig. 4C, D).

Evaluate the Efficiency of Integrating the Radiomics Signature Model and Clinical Model

The survival prediction performance of the model using iAUC indicated that the radiomics model was likely to become an independent parameter in survival prediction in all four data sets. The prediction of overall survival efficiency is significantly increased when combining the radiomics model and clinical model. In lung 1 training set, overall survival iAUC of radiomics model and clinical models were 0.615 (95% CI 0.584, 0.646) and 0.549 (95% CI 0.511, 0.587), respectively. When compared between the radiomics and clinical models, the iAUC difference is 0.066 (95% CI, 0.016, 0.116); $p = 0.0082$. Combine of radiomics model with the clinical model increased iAUC to 0.621 (95% CI 0.588,

Table 3 Model performances measured by iAUC in the overall survival prediction

Model	iAUC	95% CI	iAUC difference	95% CI	*p*
Lung 1 training set					
Radiomics	0.615	0.584–0.646			
Clinical	0.549	0.511–0.587			
Radiomics + clinical	0.621	0.588–0.654			
Radiomics + clinical vs. radiomics			0.006	−0.019–0.032	0.657
Radiomics + clinical vs. clinical			0.072	0.037–0.107	< 0.001***
Radiomics vs. clinical			0.066	0.016–0.116	0.0082**
Lung 2 testing set					
Radiomics	0.586	0.493–0.679			
Clinical	0.687	0.600–0.775			
Radiomics + clinical	0.736	0.654–0.819			
Radiomics + clinical vs. radiomics			0.150	0.055–0.245	0.0018**
Radiomics + clinical vs. clinical			0.049	−0.009–0.106	0.09
Radiomics vs. clinical			−0.101	−0.239–0.036	0.149
Kidney external validation set					
Radiomics	0.719	0.598–0.84			
Clinical	0.761	0.621–0.901			
Radiomics + clinical	0.834	0.722–0.946			
Radiomics + clinical vs. radiomics			0.116	0.004–0.227	0.041 *
Radiomics + clinical vs. clinical			0.073	−0.018–0.165	0.12
Radiomics vs. clinical			−0.042	−0.209–0.125	0.634
Head & neck external validation set					
Radiomics	0.643	0.563–0.722			
Clinical	0.693	0.614–0.771			
Radiomics + clinical	0.732	0.655–0.809			
Radiomics + clinical vs. radiomics			0.089	0.016–0.163	0.016*
Radiomics + clinical vs. clinical			0.039	−0.013–0.091	0.149
Radiomics vs. clinical			−0.05	−0.151–0.051	0.331

0.654); this model compared with Radiomics model, iAUC difference is 0.006 (95% CI −0.019, 0.032]; $p = 0.657$; and compared with clinical model having iAUC difference is 0.072 (95% CI −0.037, 0.107); $p < 0.001$ (Table3).

Overall survival iAUC of radiomics model in lung 2 testing set showed not quite high result (0.586 [95% CI 0.493, 0.679]). However, predictive performance increases when combined with clinical model (0.736 [95% CI 0.654, 0.819]).

In two external validation sets, the model performances measured by iAUC showed positive results that all the models (radiomics, clinical, and radiomics + clinical) can participate in overall survival prediction. In head and neck external validation set, overall survival iAUC of radiomics, clinical, and radiomics + clinical models were 0.643 (95% CI 0.563, 0.722), 0.693 (95% CI 0.614, 0.771), and 0.732 (95% CI 0.655, 0.809), respectively. Kidney external validation set shows result of overall survival iAUC of radiomics, clinical, and radiomics + clinical models which were 0.719 (95% CI 0.598, 0.84), 0.761 (95% CI 0.621, 0.901), and 0.834 (95% CI 0.722, 0.946) (Table 3).

In all three data sets, lung 2 testing set, head and neck validation set, and kidney validation set, when compared between radiomics-only and clinical + radiomics model, the iAUC differences were 0.150 (95% CI, 0.055, 0.245), $p = 0.0018$; 0.089 (95% CI, 0.016, 0.163), $p = 0.016$; and 0.116 (95% CI, 0.004, 0.227], $p = 0.041$, respectively; all show a significant difference (Table 3).

The radiomics + clinical model exhibited the best iAUC (Fig. 5) and fewer prediction errors and showed lower prediction errors when compared to the reference model in all data sets (Fig. 6).

Discussion

Cancer tumors in different organs might share some common image characteristic; our study learned to find the CT-based radiomics signatures trained from one cancer data set in one specific organ (NSCLC patients in lung 1 training set) that can be applied to other organs (RCC in kidney external

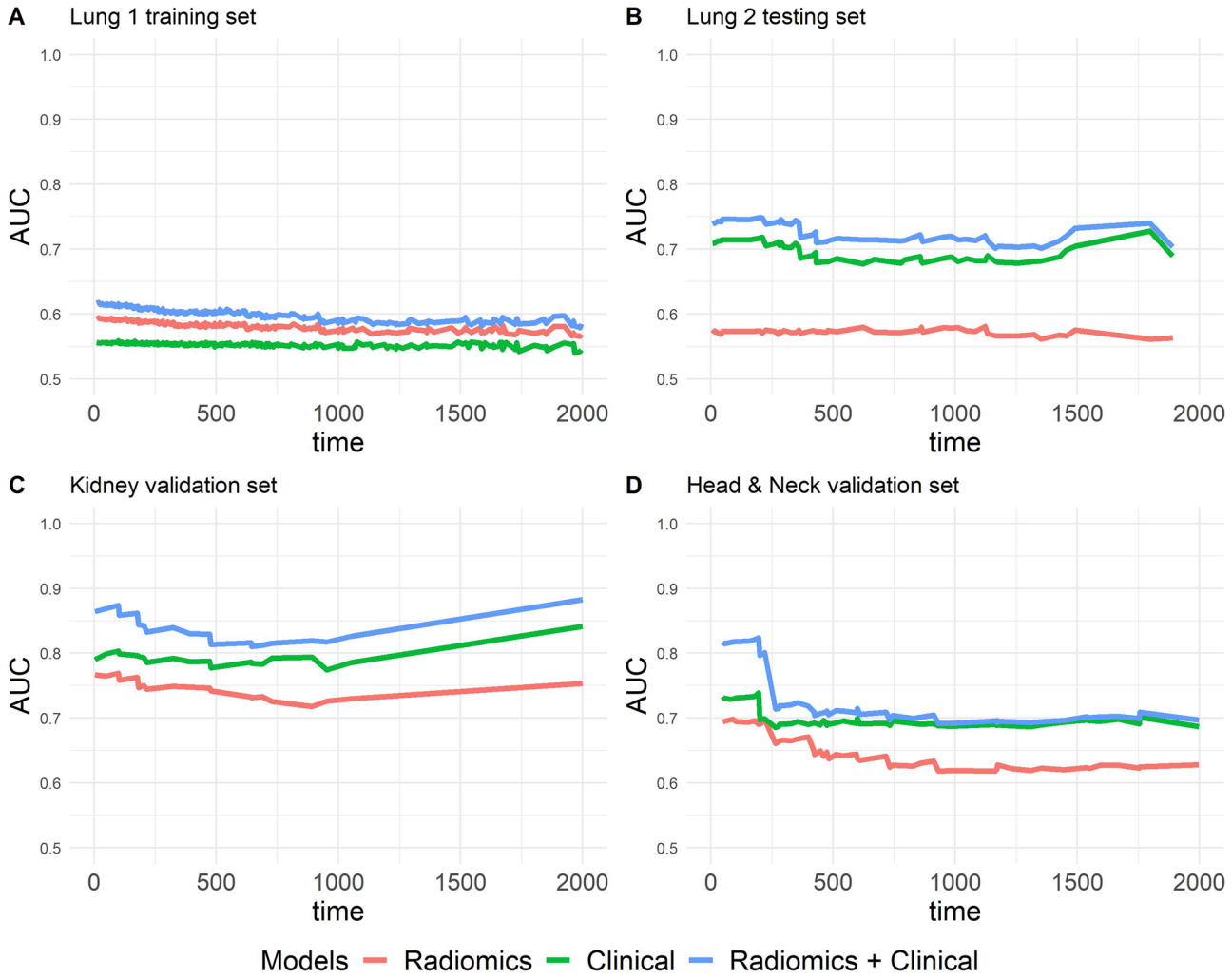

Fig. 5 Time-dependent area under the curves. **A** Lung 1 training set. **B** Lung 2 testing set. **C** Kidney validation set. **D** Head and neck validation set

validation set and SCC in head and neck external validation set). In this work, we built the risk score generated from ten radiomics signatures on lung 1 training set, between high-risk and low-risk individuals; the Kaplan–Meier curve revealed a substantial difference in survival time similar to previous study [39], then we applied on three other data sets representing three cancers in 3 locations: NSCLC patients in lung 2 testing set, RCC patients in kidney external validation set, and HNSCC patients in head and neck external validation set and results show that 1 CT-based radiomics signature that training in NSCLC patient data set also plays a role in predicting survival for two other organs. A study by Aerts et al. [23] also shows the same results when the radiomics signature built on the same data set of lung 1 plays a similar role in predicting the SCC patients' survival in the head neck 1 data set. Xu et al. [24] also studied 2D and 3D radiomics signature sets across multiple organs; however, their study just used 2D and 3D features; in contrast, our study uses all groups of radiomics features (i.e., shape, textures, intensity, and wavelet); the more features, the better the chance to find features that share the same characteristics in cancers of different organs; thus, the possibility of acquiring a set of radiomics signatures that are specific to cancer at multiple sites will increase. Another author had a similar study compared with us; Lee et al. [25] built a set of radiomics signatures on three organs: lung, kidney, and brain, but only lung and kidney radiomics features were extracted from CT, another extracted from MRI; this study has the result that a set of radiomics signatures that trained on the lung data set cannot be used to predict survival in another organ cancer (kidney, brain); our results are in contrast to this author, which can explain the difference in the data set we used, so our study itself needs to be applied to more organ and more data sets to attest to the effectiveness of our research.

To further evaluate the efficacy of one CT-based radiomics signature set for overall survival prediction in our study,

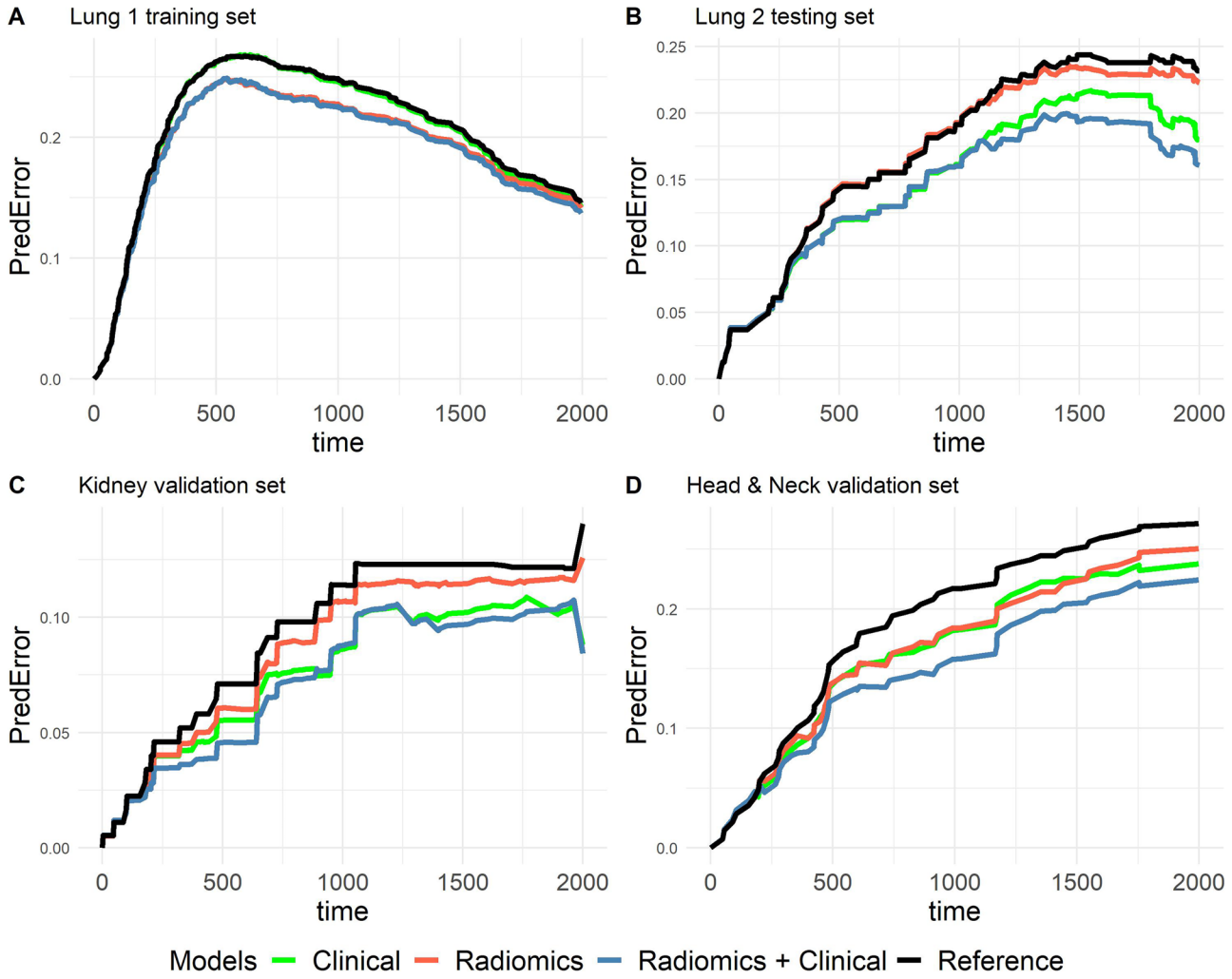

Fig. 6 Predictor error curves of multivariable Cox models. **A** Lung 1 training set. **B** Lung 2 testing set. **C** Kidney validation set. **D** Head and neck validation set`

in multivariable Cox proportional hazards, model performance was measured (iAUC) for overall survival prediction. Firstly, the radiomics signatures can stand alone when predicting survival through three different organ cancers. In the lung 1 training set, the iAUC value demonstrated that the radiomic model outperformed the clinical model (age, stage, and gender) in terms of prediction; Li et al. [36] and the previous study [14] showed a similar result, through our testing set (lung 2) and external validation set (kidney and head and neck data sets), we found that radiomics model standing alone had a lower predictive value than clinical parameters (age, gender, and stage). Furthermore, combining radiomics models with clinical parameters, the performance increased and was the highest among the three models we used in the study. Our result is similar to some previous studies. Mo et al. [40] have the result that the combination radiomic–clinical model performed well in risk prediction of progression-free survival in hypo-pharyngeal cancer patients who were having chemo-radiotherapy. Khodabakhshi et al. [4] showed that combination model (clinical and radiomic) outperforms the clinical model in overall survival prediction in renal cell carcinoma. The XG-Boost model, which combines radiomic features and clinical information, performed better than the other prediction models for overall survival prediction in RCC patients, followed by the study of Nazari et al. [19]. Other studies on brain cancer also show that combined models (radiomics + clinical model, radiomics + clinical + gene model) often give better predictive performance than individual models [33, 34].

Despite these encouraging results, significant limitations remain. First, because our findings were confined to three organs (lung, kidney, and head and neck), future research could expand on this method to include more organs. Second, our study found that the radiomics model itself has the ability to independently predict survival proven through multiple organs data set; furthermore, when the radiomics

model is combined with other models, specifically in this study when combined with clinical model, results showed an increase in predictive efficiency although in some data sets this increase was not statistically significant. In future studies, if there are more data, for example, gene data or more clinical variables such as pathology and treatment methods, we think that combining models will give significantly increased efficiency when compared to single models (radiomics model). Third, this study's data derives from several sources (lung 1-radiomics, lung 2 radio-genomics, head-and-neck squamous cell carcinoma (HNSCC), Kidney Tumor Segmentation Challenge (KiTS19)) so that the characteristics of CT images, initial image processing, segmentation, and so on differed (Table 1) that may affect our results. However, to extract features from this data, we utilized the 3D Slicer software and the pyradiomics package (satisfied the IBSI standards), which only partially guarantees the study's conclusions. Still, somehow, these methods may not ultimately ensure that the radiomics features generated from these four data sets are harmonized. Texture features are particularly affected by CT scan acquisition parameters, so to avoid biases that may affect research results, we wish to analyze similar experiments on the data sets with the same CT acquisition technique, same institution, same machine, and same reconstruction filter in our future study. Fourth, the effect of adding radiomics model to clinical data varies, sometimes adding a minor benefit and other times adding a more significant benefit; maybe, our results are affected by some bias of the data's original characteristics which come from several different sources.

Conclusion

We think that there is a possibility that the CT-based radiomics signatures may predict overall survival in different sites of cancers. Further studies are required on a range of other different organs to support this hypothesis. CT-based radiomics signatures in NSCLC overall survival prediction also show the potential to be an independent predictor for overall survival prediction in other sites of cancers, and when combined with conventional clinical parameters, radiomics improved the prognostic value for predicting survival in different malignant tumors.

Supplementary Information The online version contains supplementary material available at https://doi.org/10.1007/s10278-023-00778-0.

Author Contribution Viet Huan Le: conceptualization, methodology, validation, formal analysis, investigation, writing—original draft preparation, visualization, Quang Hien Kha: validation, investigation, data curation, writing—original draft preparation, visualization, Tran Nguyen Tuan Minh: investigation, data curation, Van Hiep Nguyen: validation, data curation, Van Long Le: validation, visualization, Nguyen Quoc Khanh Le: conceptualization, methodology, validation, writing—review and editing, supervision, funding acquisition, All authors have read and agreed to the published version of the manuscript.

Funding This work was supported by the National Science and Technology Council, Taiwan (grant numbers MOST110-2221-E-038–001-MY2 and MOST111-2628-E-038–002-MY3), and the Taiwan Higher Education Sprout Project by the Ministry of Education (grant number DP2-111–21121-01-A-12).

Data Availability All datasets are publicly available at The Cancer Imaging Archive (TCIA) (https://www.cancerimagingarchive.net/). The first cohort, Lung 1 (NSCLC-Radiomics): https://doi.org/10.7937/K9/TCIA.2015.PF0M9REI. The second cohort, Lung 2 (NSCLC Radiogenomics): http://doi.org/10.7937/K9/TCIA.2017.7hs46erv. The third cohort, Head-Neck-Radiomics-HN1: https://doi.org/10.7937/tcia.2019.8kap372n. The fourth cohort, Training Set of the 2019 Kidney and Kidney Tumor Segmentation Challenge (KiTS19): https://doi.org/10.7937/TCIA.2019.IX49E8NX Source codes for analyses are made available online at https://github.com/huanlevietMD/Overall-survival-prediction-in-multi-organ-cancer.

Declarations

Conflict of Interest The authors declare no competing interests.

References

1. Sung, H., et al., *Global Cancer Statistics 2020: GLOBOCAN Estimates of Incidence and Mortality Worldwide for 36 Cancers in 185 Countries.* CA Cancer J Clin, 2021. **71**(3): p. 209-249.
2. Hoffman, P.C., A.M. Mauer, and E.E. Vokes, *Lung cancer.* Lancet, 2000. **355**(9202): p. 479-485.
3. Pearson, F.G., *Non-small cell lung cancer: role of surgery for stages I-III.* Chest, 1999. **116**: p. 500S-503S.
4. Khodabakhshi, Z., et al., *Overall Survival Prediction in Renal Cell Carcinoma Patients Using Computed Tomography Radiomic and Clinical Information.* J Digit Imaging, 2021. **34**(5): p. 1086-1098.
5. Pulte, D. and H.J.T.o. Brenner, *Changes in survival in head and neck cancers in the late 20th and early 21st century: a period analysis.* Oncologist, 2010. **15**(9): p. 994.
6. Aerts, H.J., *The Potential of Radiomic-Based Phenotyping in Precision Medicine: A Review.* JAMA Oncol, 2016. **2**(12): p. 1636-1642.
7. GGillies, R., P. Kinahan, and H. Hricak, *Radiomics: Images Are More than Pictures, They Are Data.* Radiology, 2016. **278**(2): p. 563–577.
8. Le, N.Q.K., et al., *Radiomics-based machine learning model for efficiently classifying transcriptome subtypes in glioblastoma patients from MRI.* Comput Biol Med, 2021. **132**: p. 104320.
9. Zhang, B., et al., *Radiomics Features of Multiparametric MRI as Novel Prognostic Factors in Advanced Nasopharyngeal Carcinoma.* Clin Cancer Res, 2017. **23**(15): p. 4259-4269.
10. Reiazi, R., et al., *The impact of the variation of imaging parameters on the robustness of Computed Tomography radiomic features: A review.* Comput Biol Med, 2021. **133**: p. 104400.
11. Luo, W.Q., et al., *Predicting Breast Cancer in Breast Imaging Reporting and Data System (BI-RADS) Ultrasound Category 4 or 5 Lesions: A Nomogram Combining Radiomics and BI-RADS.* Sci Rep, 2019. **9**(1): p. 11921.
12. Liu, X., et al., *Multiregional-Based Magnetic Resonance Imaging Radiomics Combined With Clinical Data Improves Efficacy in*

Predicting Lymph Node Metastasis of Rectal Cancer. Front Oncol, 2020. **10**: p. 585767.
13. Chiesa-Estomba, C.M., et al., *Radiomics and Texture Analysis in Laryngeal Cancer. Looking for New Frontiers in Precision Medicine through Imaging Analysis.* Cancers (Basel), 2019. **11**(10).
14. Le, V.-H., et al., *Risk Score Generated from CT-Based Radiomics Signatures for Overall Survival Prediction in Non-Small Cell Lung Cancer.* Cancers (Basel), 2021. **13**(14): p. 3616.
15. Soufi, M., H. Arimura, and N. Nagami, *Identification of optimal mother wavelets in survival prediction of lung cancer patients using wavelet decomposition-based radiomic features.* Med Phys, 2018. **45**(11): p. 5116-5128.
16. Sun, W., et al., *Effect of machine learning methods on predicting NSCLC overall survival time based on Radiomics analysis.* Radiat Oncol, 2018. **13**(1): p. 1-8.
17. Peng, Z., et al., *Application of radiomics and machine learning in head and neck cancers.* Int J Biol Sci, 2021. **17**(2): p. 475.
18. Yuan, Y., et al., *MRI-based radiomic signature as predictive marker for patients with head and neck squamous cell carcinoma.* Eur J Radiol, 2019. **117**: p. 193-198.
19. Nazari, M., I. Shiri, and H. Zaidi, *Radiomics-based machine learning model to predict risk of death within 5-years in clear cell renal cell carcinoma patients.* Comput Biol Med, 2021. **129**: p. 104135.
20. Yip, S.S. and H.J. Aerts, *Applications and limitations of radiomics.* Phys Med Biol, 2016. **61**(13): p. R150-66.
21. Baba, A.I. and C. Câtoi, *Comparative oncology*. 2007: Publishing House of the Romanian Academy Bucharest.
22. García-Figueiras, R., et al., *How clinical imaging can assess cancer biology.* Insights Imaging, 2019. **10**(1): p. 1-35.
23. Aerts, H.J., et al., *Decoding tumour phenotype by noninvasive imaging using a quantitative radiomics approach.* Nat Commun, 2014. **5**: p. 4006.
24. Xu, L., et al., *A multi-organ cancer study of the classification performance using 2D and 3D image features in radiomics analysis.* Phys Med Biol, 2019. **64**(21): p. 215009.
25. Lee, S.H., et al., *Are radiomics features universally applicable to different organs?* Cancer Imaging, 2021. **21**(1): p. 31.
26. Clark, K., et al., *The Cancer Imaging Archive (TCIA): maintaining and operating a public information repository.* J Digit Imaging, 2013. **26**(6): p. 1045-1057.
27. Bakr, S., et al., *A radiogenomic dataset of non-small cell lung cancer.* Sci Data, 2018. **5**: p. 180202.
28. Heller, N., et al., *The state of the art in kidney and kidney tumor segmentation in contrast-enhanced CT imaging: Results of the KiTS19 challenge.* Med Image Anal, 2021. **67**: p. 101821.
29. van Griethuysen, J.J.M., et al., *Computational Radiomics System to Decode the Radiographic Phenotype.* Cancer Res, 2017. **77**(21): p. e104-e107.
30. Sugai, Y., et al., *Impact of feature selection methods and subgroup factors on prognostic analysis with CT-based radiomics in non-small cell lung cancer patients.* Radiat Oncol, 2021. **16**(1): p. 80.
31. Shukla, S., et al., *Development of a RNA-Seq Based Prognostic Signature in Lung Adenocarcinoma.* J Natl Cancer Inst, 2017. **109**(1).
32. Chen, H.-Y., et al., *A five-gene signature and clinical outcome in non–small-cell lung cancer.* N Engl J Med, 2007. **356**(1): p. 11-20.
33. Bae, S., et al., *Radiomic MRI Phenotyping of Glioblastoma: Improving Survival Prediction.* Radiology, 2018. **289**(3): p. 797-806.
34. Choi, Y., et al., *Radiomics may increase the prognostic value for survival in glioblastoma patients when combined with conventional clinical and genetic prognostic models.* Eur Radiol, 2021. **31**(4): p. 2084-2093.
35. Wang, X., et al., *Can peritumoral radiomics increase the efficiency of the prediction for lymph node metastasis in clinical stage T1 lung adenocarcinoma on CT?* Eur Radiol, 2019. **29**(11): p. 6049-6058.
36. Li, H., et al., *CT-Based Radiomic Signature as a Prognostic Factor in Stage IV ALK-Positive Non-small-cell Lung Cancer Treated With TKI Crizotinib: A Proof-of-Concept Study.* Front Oncol, 2020. **10**: p. 57.
37. Kim, M.-J., et al., *Early risk-assessment of patients with nasopharyngeal carcinoma: the added prognostic value of MR-based radiomics.* Transl Oncol, 2021. **14**(10): p. 101180.
38. Blanche, P., J.-F. Dartigues, and H. Jacqmin-Gadda, *Estimating and comparing time-dependent areas under receiver operating characteristic curves for censored event times with competing risks.* Stat Med, 2013. **32**(30): p. 5381-5397.
39. Yang, L., et al., *Development of a radiomics nomogram based on the 2D and 3D CT features to predict the survival of non-small cell lung cancer patients.* Eur Radiol, 2019. **29**(5): p. 2196-2206.
40. Mo, X., et al., *Prognostic value of the radiomics-based model in progression-free survival of hypopharyngeal cancer treated with chemoradiation.* Eur Radiol, 2020. **30**(2): p. 833-843.